Mon. Not. R. Astron. Soc. **000**, 000–000 (0000) Printed 26 November 2008 (MN LATEX style file v2.2)

Cosmological parameters after WMAP5: forecasts for Planck and future galaxy surveys

L.P.L. Colombo[1], E. Pierpaoli[1], & J.R. Pritchard [2⋆]

[1] *University of Southern California, Los Angeles, CA, 90089-0484*
[2] *Harvard-Smithsonian Center for Astrophysics, 60 Garden St., Cambridge, MA 02138*

Accepted ???. Received ???; in original form ???

ABSTRACT

With its increased sensitivity and resolution, the Planck satellite is expected to improve the measurement of most cosmological parameters by several factors with respect to current WMAP results. The actual performance however, may depend upon various aspects of the data analysis. In this paper we analyse the impact of specifics of the data analysis on the actual final results. We also explore the synergies in combining Planck results with future galaxy surveys. We find that Planck will improve constraints on most cosmological parameters by a factor 3–4 and on the tensor–to–scalar ratio r by a factor 9. Also inflationary parameters, like r, $n_{\rm s}$ and n_{run}, are practically not degenerate any longer. The tensor spectral index, however, is little constrained. A combination of the 70 to 143 GHz channels will contain about 90% of all possible information, with 143 GHz polarisation information carrying about half of the constraining power on r. Also, the error on r degrades by a factor 2 if no B modes are considered in the analysis. High–l temperature information is essential for determination of $n_{\rm s}$ and $\Omega_{\rm b}$, while improving noise properties increase the l–range where Planck would be cosmic variance limited in polarisation, implying a significant improvement on the determination of r, τ and A_s. However, a sub-percent difference in the FWHM used in the data analysis with respect to the one in the map will result in a bias for several parameters. Finally, Planck will greatly help future missions like LSST and CIP reach their potentials by providing tight constraints on parameters like $n_{\rm s}$ and n_{run}. Considering Planck together with these probes will help in breaking degeneracies between $\Omega_{\rm K}$ and Ω_Λ or $\Omega_{\rm dm}$ and f_ν, resulting in improvements of several factors in the error associated to these parameters.

Key words:
cosmic microwave background – cosmological parameters – galaxies: statistics – cosmology: large–scale structure of the Universe

1 INTRODUCTION

Observations of the cosmic microwave background (CMB) have driven an incredible improvement in our understanding of the Universe in the last few decades. The discovery of CMB anisotropies by the COBE satellite triggered the planning of new space missions targeted to the study of CMB anisotropies: WMAP and Planck. The WMAP satellite has already delivered results and is still flying, while the Planck satellite is scheduled to fly next year. It is therefore appropriate at this time to use the experience acquired with the WMAP data analysis in order to gain information on what can be expected in terms of parameter determination from Planck.

Given the improved technical performances, Planck carries great expectations and several authors have proposed a plethora of models that should be constrained with the new Planck data (e.g. Bond et al. 2004; Burigana et al. 2004; Perotto et al. 2006; White 2006; Balbi 2007; Xia et al. 2007; Gratton et al. 2008; La Vacca & Colombo 2008). In general, these estimates aim at an extended set of parameters beyond the minimal cosmological model, but rely on a number of simplifying assumptions. Actual constraints will depend sensitively on the ability of Planck to clean foregrounds from individual frequency channels, maximising the cosmological information available.

In this paper, we adopt a different perspective focusing on quite simple cosmological models and then exploring the required Planck performance needed for useful constraints. We explore the effects of foreground cleaning restricting the frequency channels and angular scales available for cosmology, and the effects of beam degradation. These have differing effects on individual parameter constraints and weakened experimental performance can en-

⋆ Hubble Fellow

hance degeneracies between parameters. These issues have been partly addressed in the Planck bluebook (The Planck Collaboration 2006). This paper is meant to provide further and more detailed information than that contained in the bluebook, especially in light of what has been learnt from WMAP. At the same time, we hope that our results are more transparent than those of full experimental simulations, which fully include experimental imperfections but are restricted in the range of parameter space explored.

Specifically, we will first consider a minimal set of parameters and perform a Monte Carlo Markov Chains (MCMC) estimate of the accuracy Planck will have in determining them, also showing under which conditions these results are attained. Then we will consider a more extended set of parameters including the possible presence of gravitational waves, curvature, neutrino–related parameters, quintessence and we will discuss how the previous results are modified in the presence of this extended set. While an appropriate treatment of Planck parameter estimation should also contain a general approach to reionisation (Mortonson & Hu 2008; Colombo & Pierpaoli 2008), in the following we will simply consider a sharp reionisation process parametrised only by the total optical depth τ. As shown in Colombo & Pierpaoli (2008), such assumption should not impact the size of errorbars for most parameters, which is the main interest of this paper. Finally, we will discuss the role of Planck as support for the success of galaxy surveys as cosmological probes. Galaxy surveys are able to constrain a subset of the cosmological parameter set, typically relying on CMB data to provide information on the remaining parameters and to significantly reduce degeneracies. Currently, no space CMB mission is planned after Planck, and therefore the combination of Planck with external datasets such as galaxy surveys will be a fundamental tool for estimating the cosmological parameters in the coming years.

The simplified procedure adopted here will by no means be the one adopted during the actual data analysis. For example, the effect of the precise sky cut applied on power spectrum estimation and likelihood evaluation (e.g., Hivon et al. 2002; Lewis et al. 2002; Brown et al. 2005), the effect of foreground residual on small and large scale (e.g., Serra et al. 2008; Betoule et al. 2008) or the effect of lensing on the polarisation power spectrum are all not investigated here (e.g., Lewis 2005; Smith et al. 2006). All these extra complications will however tend to degrade the level of performance for the Planck satellite. The results presented here should therefore be considered as a target or an optimistic limit.

This paper is organised as follows: in section 2 we will present the method and apply it to a configuration mimicking the WMAP 5 yrs data release; in section 3 we will discuss the performances expected for Planck for different frequency combinations and sets of parameters; section 4 is dedicated to investigating the role of Planck as support for other missions and finally section 5 is dedicated to the conclusions.

2 METHOD AND WMAP–5YR CASE

In this paper we will perform a MCMC analysis of simplified mock data to estimate Planck performances in parameter estimation, using the CosmoMC package[1] (Lewis & Bridle 2002) The availability of fast codes for evaluation of CMB power spectra, e.g. PICO[2] (Fendt & Wandelt 2007), allows good convergence of the chains to be obtained in $\sim$ 1h on modern office workstations, thus providing a valid alternative to a Fisher matrix approach, while avoiding some of the Fisher matrix shortcomings (see, e.g., Perotto et al. 2006, for a more in depth comparison of MCMC and Fisher matrix approaches).

Specifically, we will consider idealistic simulations of CMB data, assuming white isotropic noise and Gaussian beams. Real data analysis will have to deal with complications like anisotropic and correlated noise, beam systematics, calibration effects. A complete treatment of these effects is beyond the scope of this paper and to some extent would require access to the actual measurements and in–flight data. In addition, we do not consider residual foreground contribution in the mock data. Rather we assume that some of the frequencies will be used to completely clean the remaining channels, which will be the only ones used for data analysis. In practice, this is the strategy adopted up to now (e.g. Dunkley et al. 2008). We will then show how our results depend on this choice of channels.

For full sky and noiseless data, the exact likelihood of a cosmological model, defined by a set of CMB angular power spectra $\mathbf{C}_\ell{}^{\rm th}$, given a simulated dataset, $\hat{\mathbf{C}}_\ell$, is given by the Wishart distribution (Percival & Brown 2006; Hamimeche & Lewis 2008). It reads

$$\log \mathcal{L}(\mathbf{C}_\ell{}^{\rm th}|\hat{\mathbf{C}}_\ell) = \quad (1)$$
$$-\frac{1}{2}\sum_\ell (2\ell+1)\left\{\mathrm{Tr}\left[\hat{\mathbf{C}}_\ell(\mathbf{C}_\ell{}^{\rm th})^{-1}\right] - \ln|\hat{\mathbf{C}}_\ell(\mathbf{C}_\ell{}^{\rm th})^{-1}| - n\right\}$$

where n is the number of different modes (T, E and B) considered. With this choice of normalisation $\log\mathcal{L}(\mathbf{C}_\ell{}^{\rm th}|\hat{\mathbf{C}}_\ell) = 0$ for $\mathbf{C}_\ell{}^{\rm th} = \hat{\mathbf{C}}_\ell$. In the presence of white noise and for an instrument with Gaussian beams, the above expression holds provided we replace $\mathbf{C}_\ell$ with $\mathbf{C}_\ell + \mathcal{N}_\ell B_\ell^2$, where $\mathcal{N}_\ell$ are the white noise spectra and B_ℓ is the spherical harmonic transform of the instrument's beam. In addition, when combining different frequencies, we use an inverse noise weighting.

In the presence of sky cuts or non–uniform noise, equation 1 is no longer exact. In this work, we approximate the effect of sky cuts by multiplying the r.h.s. in equation 1 by a factor $f_{\rm sky}^2$, where $f_{\rm sky}$ is the fraction of sky actually observed. This *ad–hoc* correction crudely accounts for the loss of statistics and the induced correlations between different multipoles, and is already implemented in CosmoMC. For Planck, we assume $f_{\rm sky} = 0.80$. This approximation is not well suited to describe the behaviour of the likelihood function at low multipoles, which are critical for the determination of cosmological parameters like the optical depth to reionisation, τ, and the tensor–to–scalar ratio, r. Features like non–uniform sky coverage alter the shape of the likelihood function, and introduce correlations between multipoles, in particular at ℓ's corresponding to scales similar to the dimensions of the cuts. A discussion of how this affect our results for r is presented in section 3.2.

As a first application, we consider the WMAP 5 yrs (WMAP5) case, introducing in the analysis the frequencies that were actually used in the real data analysis at different scales. In particular, we adopted V and W bands in temperature and Ka,Q and V bands for large scale polarisation reducing to Q and V only for small scale polarisation. For WMAP we considered 75% sky coverage, according to the mask applied by the WMAP team to the actual observed maps, and an average noise value for each frequency considered computed from such maps. We do not consider the effect of lensing or marginalisation over the amplitude of the Sunayev-Zeldovich template.

The results are summarised in table 1, where we report the

[1] http://cosmologist.info/cosmomc/
[2] http://cosmos.astro.uiuc.edu/pico/

	Percentage difference	Ratio to Planck
$\omega_{\rm b}$	0.22	3.9
$\omega_{\rm c}$	0.38	3.2
τ	0.33	2.5
$n_{\rm s}$	0.16	4.6
$\mathcal{A}_{\rm s}$	0.31	2.4
r	0.33	9.1
H_0	0.23	3.9

Table 1. Comparison of uncertainties from actual WMAP 5–year data analysis and MCMC estimates. Table shows the percentage difference $1-\sigma_{\rm MCMC}/\sigma_{\rm WMAP}$ for the basic ΛCDM + tensor model. The third column shows the MCMC estimates of the standard deviation in unit of the expected Planck accuracy, assuming cleaning of the 70, 100 and 143 GHz channels (see table 3).

	LFI			HFI		
Central Frequency	30	44	70	100	143	217
Angular Resolution (arcmin)	33	24	14	9.5	7.1	5.0
$\Delta T/T$ per pixel (I)	2.0	2.7	4.7	2.5	2.2	4.8
$\Delta T/T$ per pixel (Q, U)	2.8	3.9	6.7	4.0	4.2	9.8

Table 2. Planck specification as reported in the Planck bluebook. Listed sensitivities are goal sensitivity assuming 14 months integration, for a square pixel with a side equal to the angular resolution of the corresponding channel.

percentage difference in the parameters' standard deviation with respect to the actual WMAP5 performances (Dunkley et al. 2008) for a ΛCDM cosmology with tensors. For comparison, we also report the expected performance of the Planck satellite, considering an ideal combination of the 70, 100 and 143 GHz channels (see below for more details). We conclude that this simplified approach in the case of WMAP5 leads to underestimate of parameters uncertainties by $25-30\%$. Although this result does not fully validate this procedure for Planck, it is encouraging that its performances on simulated WMAP5 data are so close to the actual measured value.

Figure 1 provides a visual comparison of our analysis applied to simulated WMAP5 and Planck data. Planck is expected to improve on this result by typically a factor 2.5 to 4, except in the case of r, whose upper limit for a fiducial model with $r=0$ shrinks by almost an order of magnitude. It is also evident that Planck will remove or strongly reduce several degeneracies which affect WMAP data, in particular those involving the optical depth to reionisation, τ. Notice that in the WMAP5 simulations we did not include the contribution of B–modes, while for Planck we also included simulated BB data. If systematics and/or foregrounds prevent Planck from measuring the cosmological BB spectrum, the expected improvement on the tensor–to–scalar ratio upper limit would be by a factor ~ 3 (see section 3.2 for a detailed discussion).

3 PLANCK–ONLY CONSTRAINTS

Planck has a noise level which is a factor 2-10 lower than WMAP5, a wider frequency coverage, and a finer angular resolution. Cosmological constraints for Planck will therefore come from a different set of scales and frequency ranges than in the case of WMAP.

In the following, we will adopt the simplified procedure outlined above to assess Planck performances under different data analysis circumstances. We will use the noise specifications derived from the bluebook, also reported in table 2.

Initially we will consider the following fiducial ΛCDM minimal model, based on WMAP5 results: flat, $\omega_{\rm b}=0.02273$, $\omega_{\rm c}=0.1099$, $\tau=0.087$, $n_{\rm s}=0.963$, $H_0=71.9$ Km/s/Mpc and no tensor perturbations. The amplitude of the scalar fluctuation spectrum, A_s, derives from the requirement that $\sigma_8=0.796$. Following CosmoMC convention, we define here the tensor–to–scalar ratio r as the ratio of the initial curvature and gravitational waves power spectra at a reference scale of $k_{\rm piv}=0.05{\rm Mpc}^{-1}$. In the rest of the paper, we define $\mathcal{A}_{\rm s}\equiv{\rm Log}(10^{10}A_s)$. In order to explore the parameter space in a more efficient way, it is useful to chose as a primary parameter the angle subtended by the sound horizon at recombination, θ. Our basic parameter set is then:

$$\{\omega_{\rm b},\omega_{\rm c},\theta,\tau,n_{\rm s},\mathcal{A}_{\rm s},r\}\ . \qquad (2)$$

Notice that we include r in the analysis, even if the fiducial model has no tensors (see section 3.2 for a discussion of models with non–zero r). With this choice of parametrisation, H_0 and σ_8 are then derived parameters.

Plots for power spectra in this minimal model are compared to the noise level and cosmic variance at different frequencies in figure 2. In temperature, all Planck channels will be "cosmic variance limited" (i.e. the noise equals the cosmic variance) in each frequency channel up to angular scales $l\simeq 800$; while the combination of all channels up to 217 GHz is cosmic variant limited up to $\ell\simeq 1000$.

The channels for which the signal–to–noise ratio (S/N) is unity at the smallest scale (of $\ell\simeq 1600$) are 143 and 217 GHz, the former having better signal to noise at larger scales and the latter at smaller scales. Combining all channels, the signal–to–noise ratio becomes unity at $\ell\simeq 1800$. These figures partly depend on the values of the reference cosmological parameters, in particular A_s. WMAP5 data constrain A_s at $\lesssim 10\%$ level; the effect of this uncertainty on the above discussion is negligible.

As for polarisation, Planck will be cosmic variance limited up to $\ell\simeq 8-12$ (cfr with $\ell=4-5$ for WMAP5), depending on the cosmological model considered and, in particular, on the details of the reionisation history. The smallest scale with S/N above unity is $\ell\simeq 800$ for a combination of channels up to 143 or 217 GHz.

In the following, we will explore how parameter constraints would vary in the case that only a subset of frequency channels could be used for extracting cosmological information.

3.1 Minimal model: results on parameters

A great advantage of multi–frequency experiments is to be able to use frequency information to subtract foreground contributions from the maps and combine the information of different channels to derive cosmological parameters. In the case of WMAP5, for instance, a great deal of leverage in parameter estimation has come from the ability to use the Ka band in polarisation on large scales.

Similarly, Planck's performance will depend upon the ability to clean foregrounds from the largest number of channels. Planck will be able to capitalise on the existing WMAP data for its lowest frequency channels, but being an experiment with higher sensitivity it may need to use its own channels to perform the job fully. The most crucial concerns, of course, arise regarding polarisation, which is currently poorly measured. As there is consensus on the fact that polarised foregrounds are minimal around 70 GHz (e.g. Samtleben et al. 2007; Gold et al. 2008), we will consider as a minimal assumption that at least the 70 GHz channel will be cleaned.

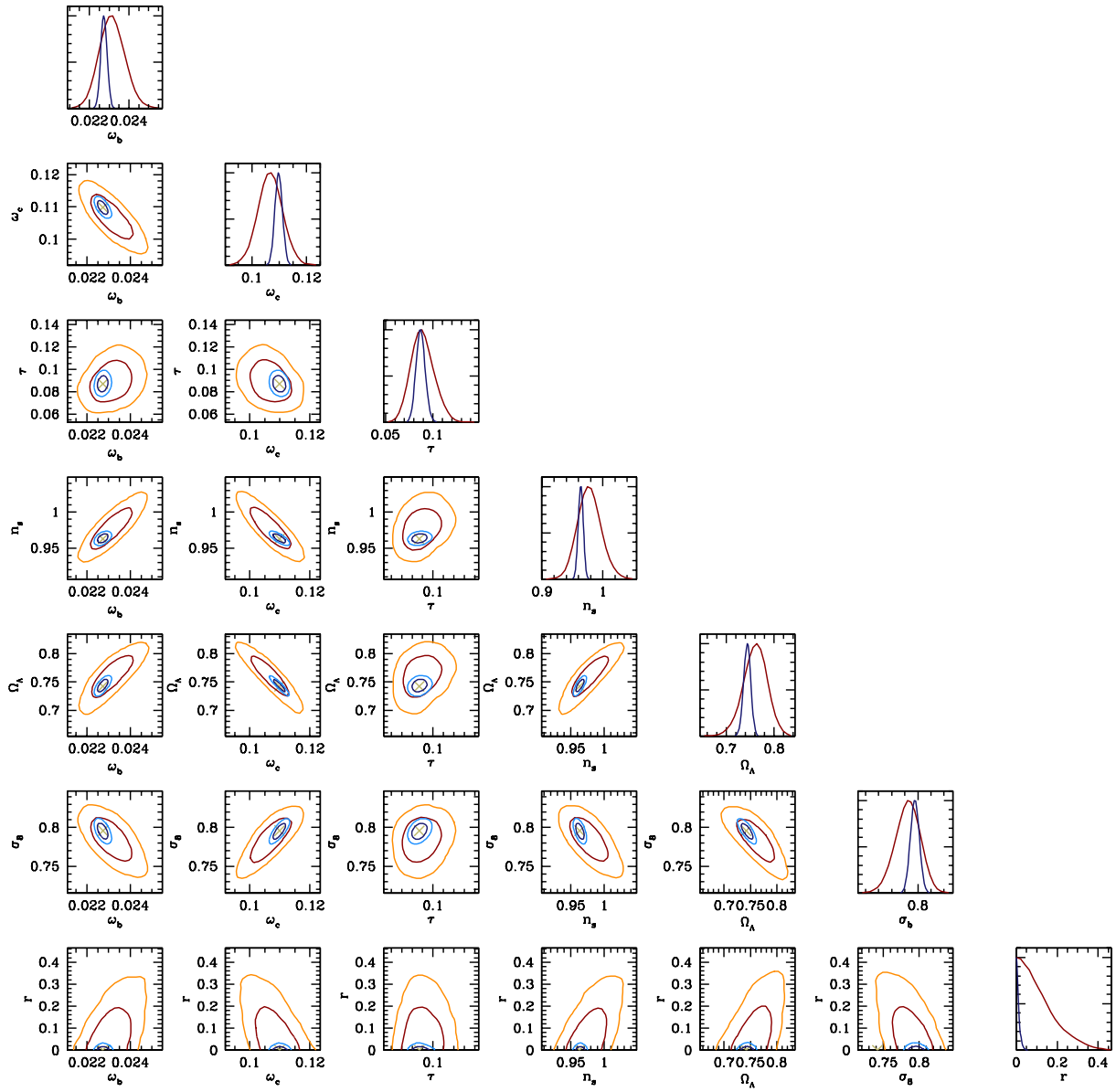

Figure 1. Marginalised distributions and joint 2D confidence regions for the base fiducial model analysed assuming a combination of 70, 100 and 143 GHz Planck channels (blue/cyan lines) or WMAP 5yr specifications (red/orange lines). The 2D plots show the 1– and 2–σ regions; crosses mark the input values for the parameters.

	70 - 143	30 - 143	70 - 100	30 - 100	70 - 143T	30 - 143T	70 - 217	30 - 217
$\omega_{\rm b}$	1.6×10^{-4}	1.00	1.50	1.48	1.20	1.18	0.87	0.86
$\omega_{\rm c}$	1.4×10^{-3}	0.99	1.37	1.33	1.23	1.19	0.90	0.90
θ	3.1×10^{-4}	1.00	1.67	1.64	1.24	1.23	0.86	0.86
τ	4.8×10^{-3}	0.97	1.25	1.17	1.23	1.15	0.95	0.92
$n_{\rm s}$	4.0×10^{-3}	0.99	1.51	1.47	1.18	1.14	0.87	0.87
$\mathcal{A}_{\rm s}$	9.5×10^{-3}	0.99	1.24	1.16	1.23	1.15	0.95	0.92
r	< 0.03	0.90	2.19	1.75	2.15	1.73	0.84	0.76
σ_8	6.7×10^{-3}	0.99	1.31	1.25	1.23	1.17	0.92	0.91
H_0	6.9×10^{-1}	0.99	1.43	1.39	1.23	1.19	0.88	0.88

Table 3. Error estimates for different combinations of Planck channels for the reference ΛCDM + tensors model. For all parameters we report the standard deviation for the marginalised distribution, except for r for which we report the upper 95% confidence limit. Second column: estimates assuming cleaning of 70, 100 and 143 GHz channels. Values shown are actual errors. Columns 3–8 shows estimates for different combinations of channels normalised to the values of column 2, when a frequency is followed by a T we only consider temperature data for that channel.

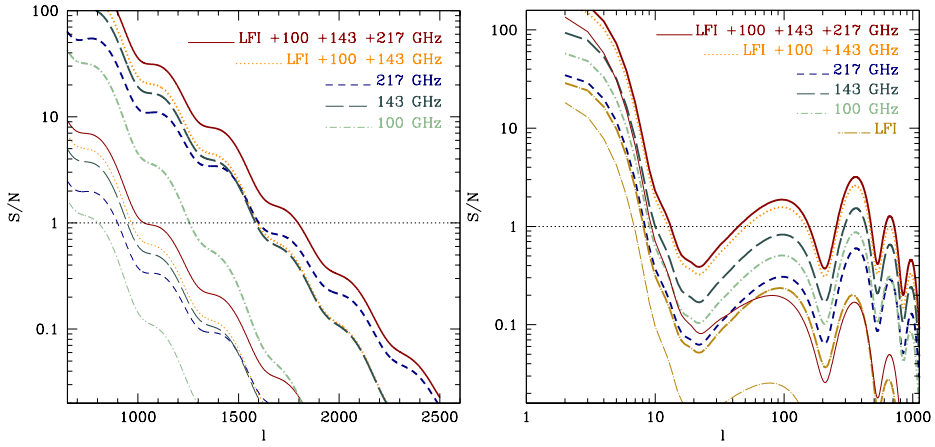

Figure 2. Planck sensitivity to the fiducial C_l spectra for different channels or channels combinations. Thick lines show the signal–to–noise ratio, thin lines show the Cosmic Variance–to–noise ratio. Left panel shows sensitivity to the TT spectrum, right panel is for the EE spectrum.

WMAP5 was not able to use the 95 GHz channel in polarisation due to potential dust contamination, however, thanks to the greater frequency coverage of Planck, we will assume that the 100 GHz channel will also be available to extract cosmological information. Starting from this minimal configuration ($70 + 100$ GHz), we will then explore the effect of adding information from higher and lower frequencies, in temperature only or both in temperature and polarisation. The results are summarised in table 3, where we quote the estimated errors on different parameters with respect to the case for the combination of channels $70 + 100 + 143$ GHz. This frequency combination is, in fact, already providing most of the information, so that adding all LFI frequencies and the 217 GHz channels would improve the results by only 10% in all parameters. The higher frequency channels would add even less, due to their higher noise level. Not being able to use the 143GHz channel in polarisation increases errors by about $15 - 25\%$ ($n_{\rm s}$ being the least impacted), except for r in which case the upper limit roughly doubles. This problem is mitigated if all LFI channels are present. Not being able to use the 143 GHz channel at all, however, would degrade the cosmological parameter determination by 20–50% on most parameter and a factor 2 on r. Also in this case, using all LFI gives $\sim 10\%$ improvement on τ and A_s while other parameters are affected at the percent level.

This simplified analysis summarises the information contained at all scales. It is indeed the case that certain foregrounds are a concern only for either temperature or polarization, or only on some spatial scales. One such example is residual point sources, which may spoil the use of small scale temperature fluctuations. It is therefore interesting to ask how much of the information comes specifically from temperature measurements and which are the relevant scales in determining each parameter. In order to address this question, we considered the 70 - 217 GHz channels combination and evaluate how much each error estimate decreases as a function of the maximum multipole $\ell_{\rm max}$ considered in the analysis. Results are compared to the case of an ideal experiment with cosmic variance limited (CVL) temperature measurements over the whole range of multipoles considered, and polarization sensitivity equal to that of the selected Planck channels. The output of this analysis is reported in figure 3.

In principle, for the minimal cosmological model considered here, Planck will recover all the relevant information on parameters encoded in the CMB power spectra up to scales $\ell \simeq 1500$, after which differences with a CVL experiment start to show. The parameters whose determination is most improved when temperature information on scales above $\ell = 800$ is included are $n_{\rm s}$, $\omega_{\rm b}$ and θ (by about 30-40%) while r, A_s and τ are basically unaffected.

While Planck will perform, in temperature, as well as a CVL experiment up to $\ell \simeq 1500$, a greater room for improvement is left for polarization measurements. This improvement may come either if Planck keeps functioning after the 14 months required to complete 2 full sky surveys, or by other ground–based or balloon–borne experiments, like the currently planned SPIDER (Crill et al. 2008). SPIDER will cover $\sim 50\%$ of the sky, with a polarization sensitivity higher than Planck, but with a lower angular resolution. It is then interesting to consider how the combination of Planck temperature measurements with better polarization data will affect cosmological parameter estimation. To asses this point we consider an ideal experiment with temperature information equal to the combination of the $70 - 217$ GHz Planck channels and CVL polarization measurements up to a multipole $\ell_{\rm CV}$ ranging between $\ell = 10$ and $\ell = 800$. Above $\ell_{\rm CV}$ polarization sensitivity is equal to that expected from Planck. Let us also point out that CVL determination of E–mode polarization above ℓ of a few hundreds will likely require the next generation of space CMB mission, like the recently proposed EPIC (Bock et al. 2008). However, if such a mission does not have high angular resolution, we do not expect a significant improvement on Planck temperature data, which are effectively CVL for $\ell \lesssim 1000$.

The right panel of figure 3 shows the improvement on parameter constraints over Planck $70 - 217$ GHz, as a function of $\ell_{\rm CV}$. As expected, a CVL determination of even the first 10 polarization multipoles would significantly improve the constrain on r. Results shown refer to a fiducial value $r = 0.05$, for which $\ell_{\rm CV} = 10$ would improve Planck constraints by a factor ~ 2; the improvement would be even more relevant for lower tensor–to–scalar ratios. While the large angle B–mode spectrum is expected to be at most comparable to Planck noise, the E–mode spectrum will be measured with essentially a CVL accuracy up to $\ell = 8 - 9$, so that $\ell_{\rm CV} = 10$ will provide only a modest, $\sim 10\%$, improvement in the determination of τ. This improvement will increase to $\sim 40\%$ if CVL data extend up to $\ell \sim 20$; above this value the polarization C_l are mostly independent of τ for the class of sharp reionisation history considered here, and further improvements on sensitivity do not lead to significant improvements on determina-

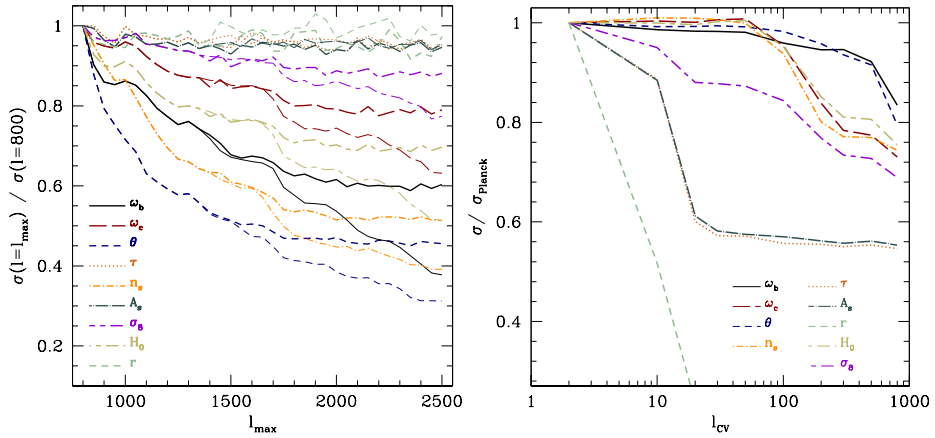

Figure 3. *Left:*Sensitivity to the different parameters as a function of the maximum multipole considered in the analysis. Plot shows error estimates for the various parameters as a function of $\ell_{\rm max}$ considered in the analysis, normalised to the error for $\ell_{\rm max} = 800$. Heavy lines are for the combination of the $70, 100, 143$ and 217GHz Planck channels, thin lines are for an ideal experiment with cosmic variance temperature measurements and polarization sensitivity equal to the Planck configuration considered here. It is clear that up to $\ell_{\rm max} \sim 1500$ a CVL experiment would not offer a significant advantage over Planck. *Right :* Impact of higher sensitivity polarization data on parameter constraints. Plot shows parameter estimates for an ideal experiment with CVL polarization data up to $\ell_{\rm CV}$ and sensitivity equal to Planck $70 - 217$ GHz channels for $\ell \geqslant \ell_{\rm CV}$. Error estimates are normalised to Planck estimates, corresponding to $\ell_{\rm CV} = 2$.

tion of the optical depth. However, the multipole range $20 - 50$ contains information on reionisation for non-minimal reionisation histories, and improving determination of this part of the spectra can significantly increase constraints on these models. Due to the $\tau - A_s$ degeneracy, the normalisation of the scalar power spectrum improves in a similar manner, which in turn affects the determination of σ_8. A second set of parameters, including $\omega_{\rm c}$, $n_{\rm s}$ and H_0, shows a $\sim 15\%$ improvement for $\ell_{\rm CV} = 100 - 200$, increasing to $\sim 25\%$ for $\ell_{\rm CV} = 800$. A third group of parameters, θ and $\omega_{\rm b}$, shows only a modest improvement for CVL data extending to the first 500 multipoles, and a $\sim 20\%$ improvement for $\ell_{\rm CV} = 800$.

In what follows, whenever not specified, we assume the frequency combination 70 + 100 + 143 GHz and include in the analysis multipoles up to $\ell_{\rm max} = 2500$, even if for Planck multipoles $\ell \gtrsim 2000$ only have a (few) percent level impact on parameter determination.

3.2 The tensor–to–scalar ratio determination

As it appears from table 1, one parameter whose determination Planck is expected to greatly improve is the tensor–to–scalar ratio r. For a fiducial model with negligible tensor contribution, $r \lesssim 0.01$ corresponding to *small–field* inflation models (for a review of inflationary physics, see Lyth & Riotto 1999), using the $70 - 143$ GHz Planck channels we expect an upper limit $r \lesssim 0.03 (95\% {\rm c.l.})$, tightening WMAP5 constraints by about 1 order of magnitude. Without the polarization information of the 143 GHz channel, this constraint degrades by more than a factor 2, while adding the 217 GHz channel would improve this figure by $\sim 15\%$. If it proves possible to use all the LFI channels for cosmological parameter estimation, the upper limit would improve by $\sim 25\%$ if the 143 GHz polarization is not included in the analysis, or by $\sim 10\%$ otherwise.

For a non–negligible, i.e. $r \gtrsim 0.05$, contribution by gravitational waves, Planck will be able to put a lower limit on r with a confidence level $\gtrsim 95\%$ (see figure 4). It is then interesting to explore to what extent results depend on the frequencies considered. Results for a fiducial cosmological model with $r = 0.05$ are given in table 4. A combination of the 70–143 GHz channels allows r to be constrained with an accuracy of $\sigma_r \sim 0.023$. The uncertainty on r increases by $\sim 50\%$ without the polarization information from the 143 GHz channel, however, since the marginalised distribution is markedly non–Gaussian even in this case it is possible to claim a 2σ detection of $r > 0$. Adding the 30 and 40 GHz channels would improve constraints on r by $10 - 15\%$. Notice that these results were obtained by fixing the tensor spectral index to $n_{\rm T} = 0$ (see below for further discussion).

The BB spectrum is a unique signature of tensor perturbation, however it is also a weaker signal than the EE and TE spectrum; it has not yet been observed, and is potentially more affected by foreground residuals. Simulations of polarised foregrounds removal strategies (Betoule et al. 2008) suggest that for Planck residual foreground contamination would increase the uncertainty on r by $\sim 30\%$, for a fiducial value $r = 0.10$. Thus, we expect foreground cleaning to have an impact on the uncertainty on r which is (at least) comparable to that of the instrumental noise. However, a detailed knowledge of polarised foregrounds is still lacking, and a correct assessment of Planck capabilities of measuring the B–mode C_ℓ will require the actual data.

For these reasons, it is sensible to ask how much of the constraining power resides in the BB measurement and to what extent the constraint on r would be weakened if instead we were only able to measure TT, EE and TE. The results are summarised in figure 4 for $r = 0, 0.05, 0.1, 0.15, 0.2$, and a fiducial set of parameters as above. In the case of a high value of r that Planck might possibly detect, not being able to use the BB spectrum would imply a doubling of the error bars, and a 3σ detection would be possible only for values $r \gtrsim 0.15 - 0.20$, in agreement with Knox & Turner (1994).

It is then clear that a significant portion of Planck's capabilities of detecting tensor modes comes from the low–ℓ part of the BB spectrum. When dealing with real data, contamination by the Galaxy, as well as component separation and point sources subtraction, will require masking of parts of the sky. In this case, the correct shape of the likelihood function is no longer given by equation 1, and for arbitrary cuts it is not possible to write an analytical expression for the likelihood in harmonic space. As discussed

above, we assumed here that it is possible to account for sky cuts simply by multiplying the Wishart distribution by a factor $f_{\rm sky}^2$. To test that this approximation does not significantly affect our determination of r, we compare it with the exact likelihood function evaluated in pixel space (we refer the interested reader to, e.g., Tegmark & de Oliveira-Costa 2001, for the relevant expressions). Evaluating the full Planck likelihood in pixel space is not numerically feasible, since it would require the inversion of a matrix with a side of $O(10^7)$ elements. However, we focus here on the determination of r which depends mainly on the $\ell \lesssim 30$ multipoles, so that we can work with low resolution maps. Using the HEALPix package[3] (Górski et al. 2005), we generate temperature and polarization maps at a resolution $N_{\rm side} = 16$, corresponding to a pixel size of ~ 3.5, including contribution by multipoles up to $\ell = 32$. We add a white noise corresponding to that expected for the $70 - 140$ GHz channels; due to the low resolution of the maps, the beam finite resolution is not relevant. From each map we remove the pixels with centers within 10 of the equator. Using the remaining pixels, corresponding $f_{\rm sky} = 0.8125$, we evaluate the exact likelihood for r, with other parameters fixed to the fiducial value. We compare this likelihood to the one evaluated with equation 1, using as fiducial spectrum the full–sky spectrum of the CMB + noise map. Both in pixel and harmonic space, we include in the likelihood evaluation TT, TE, EE and BB multipoles up to $\ell = 32$. We repeat this test for two fiducial values $r = 0$ and $r = 0.10$, for each value we perform 50 sky realization. For $r = 0$ we compare the 95% upper limits of the pixel and harmonic based likelihood, and find that in average the approximate likelihood we use throughout this work overestimates the correct result by $\sim 4\%$. For $r = 0.10$, we instead compare the variance of the two sets of distributions; using the approximate likelihood overestimates the correct results by $\sim 11\%$. As expected, when considering single realizations, the estimate of r obtained with the rescaled Wishart distribution are different from that obtained in pixel space, as the former likelihood peaks at the full–sky power spectrum, while the latter correctly takes into account only the observed portion of the sky. On average this discrepance is $\sim 0.35\sigma_r$. Elsewhere in this work we build the mock data using the theoretical power spectrum, instead of considering realizations, therefore there is no bias in the corresponding results. Since r is not significantly degenerate with the remaining parameters, with the exception of $n_{\rm T}$, we expect that these conclusions hold also when fitting for the remaining cosmological parameters, and that results of this paper do not significantly depend on the sky coverage of actual data.

3.3 Beam degradation

Planck results will come from a combination of high sensitivity and fine angular resolution. While a comparison of Planck with a CVL experiment gives an assessment of the relevance of high sensitivity, a crude test of the impact of angular resolution can be made by comparing Planck's expected performance with that of an ideal experiment with *ad–hoc* increased beam FWHM at all frequencies by either 10% or 30%.

Table 5 reports the parameter uncertainties for such an experiment, relative to the Planck expected performances quoted in table 3. An increase of 10% in FWHM worsen the constraints on most parameters by $\sim 5\% - 10\%$, while degrading the beams by 30% increases error estimates by $\sim 10\% - 20\%$, for our basic configuration. As shown in figure 5, some parameters, most noticeably $n_{\rm s}$, $\omega_{\rm b}$ and θ, gain constraining power from the measurements of high–ℓ TT power spectrum.

Real beams can be affected by a number of systematic effects, e.g. deviations from Gaussianity or asymmetries. A full assessment of these effects will require in–flight beam calibration, and is outside of the scope of this paper. Here instead, we perform a simple test of beam impact on parameter estimation by assuming that the Gaussian FWHM used in the analysis is different (either bigger or smaller) by the actual FWHM by 0.05% or 0.20%, for all frequencies considered. The major impact of a beam mismatch is a bias on most cosmological parameters, as shown in figure 6. Even an error of 0.05% in the assumed beams leads to a bias of $\sim 0.5\sigma$ on most parameters, increasing to more the $\sim 2\sigma$ for a misestimate of the FWHM by 0.20%. For Gaussian beams, the beam transfer function depends on a single ℓ. Thus, if the beam mismatch becomes relevant only at scales $\ell \gtrsim 1800 - 2000$, it is expected to affect parameter estimation at the few percent level (see figure 3). Real systematics, however, will also introduce correlations between different multipoles so in general it will not be possible to reduce these effects by simply excluding this range of ℓ's.

	70 - 143	70 - 100	70 - 143T	70 - 217
$\omega_{\rm b}$	1.6×10^{-4}	1.55	1.20	0.89
$\omega_{\rm c}$	1.4×10^{-3}	1.38	1.21	0.88
θ	3.1×10^{-4}	1.69	1.25	0.87
τ	4.9×10^{-3}	1.24	1.24	0.94
$n_{\rm s}$	4.1×10^{-3}	1.58	1.17	0.85
$\mathcal{A}_{\rm s}$	9.8×10^{-3}	1.22	1.23	0.95
r	2.3×10^{-2}	1.52	1.50	0.85
σ_8	6.9×10^{-3}	1.29	1.22	0.91
H_0	7.0×10^{-1}	1.45	1.21	0.87

Table 4. As table 3, but assuming a non–zero tensor amplitude, $r = 0.05$. In this case for r we quote the standard deviation as done with all the other parameters.

	FWHM = 1.1 FWHM$_{\rm Planck}$	FWHM = 1.3 FWHM$_{\rm Planck}$
$\omega_{\rm b}$	1.07	1.20
$\omega_{\rm c}$	1.03	1.10
θ	1.08	1.25
τ	1.00	1.01
$n_{\rm s}$	1.05	1.16
$\mathcal{A}_{\rm s}$	1.00	1.00
r	0.99	1.00
σ_8	1.03	1.06
H_0	1.05	1.14

Table 5. Error estimates for an experiment with sensitivity equal to Planck 70-143GHz channels and larger beams. Values are quoted relative to Planck estimates reported in table 3.

3.4 Away from the minimal model

After having explored Planck's performance for the minimal cosmological model, we now broaden the parameter space and investigate performance for a series of less minimal but still quite general cosmological models. These will include a running spectral index,

[3] http://healpix.jpl.nasa.gov/

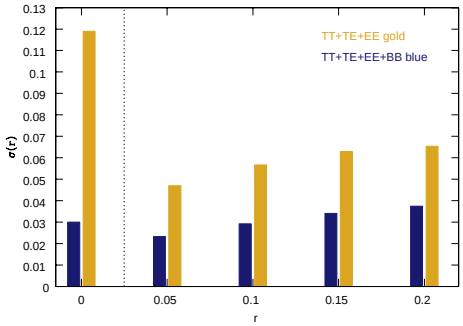

Figure 4. Impact of B–modes detection on the determination of the tensor–to–scalar ratio, r, for different fiducial values of r. For $r > 0$ bars show the expected 1σ error on the tensor–to–scalar ratio including (blue) or excluding (gold) B–modes in the analysis. For a fiducial $r = 0$ bars show the upper 95% c.l. instead. If B–modes information is not available, error on r increase by a factor ~ 2. Notice that for $r \lesssim 0.10$, the corresponding marginalised distribution is markedly non–Gaussian and quoting the standard deviation does not properly characterise the 1σ confidence interval. Results shown are for the $70 - 143$ GHz channels combination.

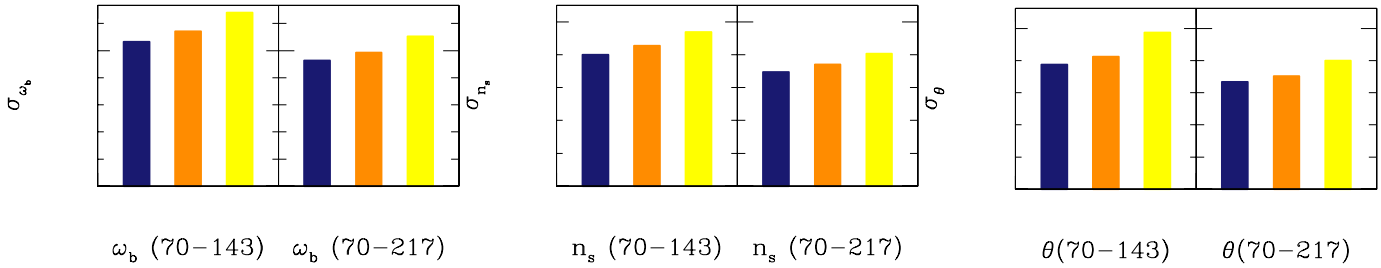

Figure 5. Impact of small angular scales on parameter determination. Histograms shows the uncertainties on $\omega_{\rm b}$, $n_{\rm s}$ and θ for nominal beams (left bar), beam enlarged by 10% (middle) or by 30% (right). For each parameter, the left panel refers to the $70 - 143$GHz channels, the right panel is for $70 - 217$ GHz channels.

neutrino–related parameters, curvature and quintessence. For these models, we will explore frequency dependence and degeneracies.

3.4.1 *Dark Energy and Cosmic Curvature*

In most cosmologies, the size of the sound horizon at last scattering provides a standard ruler at a redshift of $z_{\rm LS} \simeq 1090$. Indeed, most information on the geometry of the Universe present in the CMB power spectra, can be summarised in terms of the redshift of photon decoupling, z_*, and of two distance ratios, the acoustic scale ℓ_A and the shift parameter R (Elgarøy & Multamäki 2007; Mukherjee et al. 2008; Komatsu et al. 2008). In principle this allows for a substantial compression of information without a significant loss of accuracy, especially when combining CMB data with external measurements. This approach however cannot be adopted when simultaneously fitting for the entire set of cosmological parameters we are considering.

The geometrical degeneracy limits how the accuracy on the spectra translates in accuracy on the cosmological parameters defining the geometry of the Universe or dark energy properties and current constraints on these parameters rely heavily on external information. We wish to investigate here to what extent this will be true for Planck as well. In particular, we will consider cosmic curvature, $\Omega_{\rm K}$, and a dark energy component with a constant equation of state, w.

Constraining the geometry of the Universe to high precision provides a weak, but important probe of inflation. Generic inflation models tend to produce a Universe completely flat except for super-horizon curvature fluctuations at the level of $\Omega_{\rm K} \sim 10^{-5}$. Although this high level of precision is likely beyond currently envisaged experiments a positive detection of curvature at a level higher than this would be a very interesting result. This would not necessarily invalidate the inflationary paradigm, since open inflation models (Linde & Mezhlumian 1995) can produce $\Omega_{\rm K} \lesssim 10^{-3}$. Measurements at this level would move towards constraining such models.

	70 - 143	70 - 100	70 - 217
$\omega_{\rm b}$	1.7×10^{-4}	1.48	0.85
$\omega_{\rm c}$	1.4×10^{-3}	1.39	0.91
θ	3.1×10^{-4}	1.64	0.85
τ	4.9×10^{-3}	1.23	0.92
$\Omega_{\rm K}$	2.3×10^{-2}	1.33	0.90
$n_{\rm s}$	4.1×10^{-3}	1.54	0.88
$\mathcal{A}_{\rm s}$	9.8×10^{-3}	1.20	0.93
r	0.031	2.43	0.83
σ_8	1.1×10^{-2}	1.35	0.91
H_0	9.2	1.15	0.93

Table 6. As table 3, but for a ΛCDM + tensor + curvature model.

Table 6 reports results when the parameter space is expanded to include $\Omega_{\rm K}$. Our default Planck configuration will constrain curvature with an accuracy of $\sigma_{\Omega_{\rm K}} \sim 0.023$, compared to an accuracy of $\sigma_{\Omega_{\rm K}} \sim 0.050$ for the WMAP5–like case (see figure 7). Allowing for curvature degrees of freedom in the analysis increases the error on H_0 by more than an order of magnitude and almost doubles the error on σ_8. As expected, other parameters are not significantly affected.

We now turn to discussing estimation of dark energy properties. The simplest way to account for dark energy is to *ad–hoc*

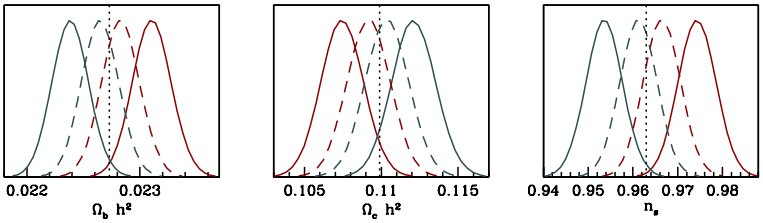

Figure 6. Effect of an incorrect beam characterisation on parameter estimation for Gaussian beams. Figure shows the bias in the recovered parameter resulting by underestimating (red lines) or overestimating (green lines) the actual beam FWHM by 0.05% (dashed lines) or 0.20% (solid).

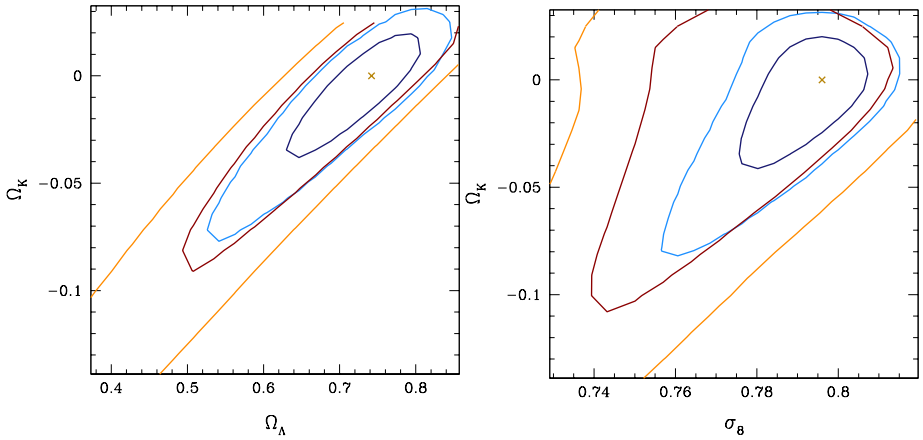

Figure 7. Joint $1-$ and $2-\sigma$ confidence regions in the $\Omega_\Lambda - \Omega_K$ (left) and in the $\Omega_\Lambda - \Omega_K$ (right) planes. Plots compare results for the $70-143$GHz channels (blue/cyan lines) with those for simulated WMAP5 data (red/orange). Crosses mark the input value of the parameters. Planck will significantly reduce the degeneracies present in WMAP5 data.

include a cosmological constant term into Einstein's equations. A more physically motivated alternative is provided by a self–interacting scalar field (Ratra & Peebles 1988; Wetterich 1988; Caldwell et al. 1998; Brax & Martin 1999). A common prediction of these models is that dark energy can be described as a perfect fluid with a time varying equation of state, $w(a)$. In general, the effects of dark energy on CMB spectra are well described by modelling dark energy as a perfect fluid with constant equation of state

$$w = \frac{\int da\, \Omega_w(a) w(a)}{\int da\, \Omega_w(a)}\ . \qquad (3)$$

This approximation is not valid for models with direct dark energy – dark matter interaction (e.g., Amendola 2000; Huey & Wandelt 2006; Mainini et al. 2005) and may lead to significant biases in the determination of cosmological parameters (Vergani et al. 2008). We will not consider the latter class of models here, and parametrise dark energy with a constant equation of state, w. We also assume a flat Universe.

Error estimates for WCDM models are quoted in table 7, while figure 8 compares degeneracy regions for Planck and WMAP in the $w-\Omega_\Lambda$ and $w-\sigma_8$ planes. As with curvature, allowing for $w \neq -1$ significantly increases the errors on H_0 and σ_8. In this case, however, estimates are not dependent on the combination of channels used, and in addition Planck provides only a marginal improvement over WMAP5. Thus, at Planck sensitivities constraints are driven by the CMB internal degeneracies and the prior used in the analysis (e.g. on H_0), rather than by the data.

In summary, Planck will significantly improve over WMAP 5–year constraints on Ω_K, but not on w. However, Planck will significantly improve over WMAP5 if we are considering models with both non–zero curvature and $w \neq -1$, or models with more than one dark energy parameter (Xia et al. 2007). In both cases, external data set will still be fundamental (also see Mukherjee et al. 2008).

	70 - 143	70 - 100	70 - 217
ω_b	1.6×10^{-4}	1.53	.897
ω_c	1.4×10^{-3}	1.40	.924
θ	3.1×10^{-4}	1.65	0.85
τ	4.8×10^{-3}	1.23	.945
w	3.5×10^{-1}	1.01	0.99
n_s	4.0×10^{-3}	1.55	.886
$\mathcal{A}_s$	9.7×10^{-3}	1.23	.953
r	0.030	2.18	.819
σ_8	1.1×10^{-2}	1.02	0.99
H_0	1.3×10	1.01	0.99

Table 7. As table 3, ΛCDM + tensor + w model. Errors on w, σ_8 and H_0 do not depend on the channels used.

3.4.2 *Neutrinos and relativistic degrees of freedom*

The detection of oscillations of solar and atmospheric neutrinos has confirmed that ν's are massive particles. However, for currently allowed values of neutrino's mass, $\sum m_\nu \lesssim 1.3$ eV (95% c.l.) (Komatsu et al. 2008), neutrinos will still be relativistic at the epoch of last scattering, so that the effective matter–to–radiation ratio at z_{LS} is lower than the matter–to–radiation ratio today. In turn, this results in a shift of the position of the first acoustic peak due to the faster decay of the gravitational potential around re-

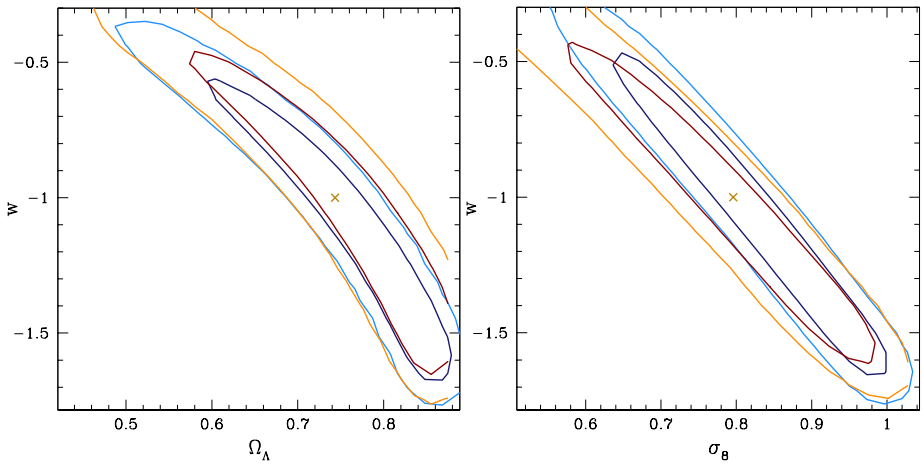

Figure 8. Joint $1-$ and $2-\sigma$ confidence regions in the $w-\Omega_\Lambda$ (left) and in the $w-\sigma_8$ (right) planes, for a combination of $70-143$ GHz Planck channels (blue/cyan lines) or for WMAP5 (red/orange lines). Cross marks the input value of the parameters. Results are dominated by intrinsic CMB degeneracies and by the choice of priors (especially on H_0).

combination, and alter the shape of the acoustic peaks (Pierpaoli 2003; Ichikawa et al. 2005; Lesgourgues & Pastor 2006). In addition, neutrino mass slightly affect the expansion rate at late times.

The three standard neutrinos may not be the only free streaming relativistic particle species present in the early Universe. Additional relativistic degrees of freedom, usually parametrised in terms of effective number of neutrino species, $N_{\rm eff}$, would push the redshift of matter–radiation equality to later epochs, which in turn affects the ratio of the heights of the first and third acoustic peaks of CMB spectra. Moreover, extra relativistic degrees of freedom change the expansion rate at early times, in particular affecting the time between (standard) neutrinos decoupling and the opening of the Deuterium bottleneck, which fixes the abundance of light elements produced in the Big Bang Nucleosynthesis. Knowledge of the Helium abundance, $Y_{\rm He}$, would then tighten constrain on $N_{\rm eff}$. WMAP5 data alone are not able to place an upper limit on $N_{\rm eff}$, even assuming $Y_{\rm He}$ is known. With its improved characterisation of the acoustic peaks, Planck is expected to significantly constrain both these parameters (also see Ichikawa et al. 2008).

Here, we discuss the determination of neutrino masses separately from that of the effective number of relativistic species and Helium abundance. We show how these constraints depend on the frequencies used, and how errors on the non–neutrinos related parameters increase with respect to results for a ΛCDM model. The fiducial cosmological model does not include massive neutrinos, $f_\nu = 0$, or additional massless species, $N_{\rm eff} = 3.04$, and $Y_{\rm He} = 0.24$.

When expanding the parameter space to include ν's mass, we assume that the three mass eigenstates are completely degenerate and parametrise the neutrino contribution to the total dark matter energy density by $f_\nu \equiv \Omega_{\nu,0}/\Omega_{{\rm dm},0}$ with $\Omega_{{\rm dm},0} \equiv \Omega_{c,0} + \Omega_{\nu,0}$. Results for the $70-143$ GHz are reported in table 8. We find an upper limit $f_\nu < 0.072$ (95% c.l.), which translates into a constraint on the sum of ν 's masses $\sum m_\nu < 0.77$ eV, according to $\sum m_\nu = 94\ {\rm eV}\,\Omega_{\nu,0}h^2 = 94\ {\rm eV} f_\nu \Omega_{{\rm dm},0}h^2$. Using only the 70 and 100 GHz channels, this limit increases by $\sim 20\%$, while if the 217GHz channel is included the limit improves by $\sim 5\%$[4]. Allowing for a contribution by massive neutrinos more than doubles the uncertainty on $\omega_{\rm dm}$ and increases errors on H_0 by ~ 3.5 times. Since σ_8 is an integrated quantity with a significant dependence on $f_\nu, \omega_{\rm dm}$ and H_0, these effects combines so that the corresponding uncertainty increase by a factor $\sim 7-8$. Errorbars on other parameters are only moderately affected, increasing by $\sim 5-10\%$, implying no significant degeneracies with f_ν. When fitting for neutrino properties, we assume a constant equation of state dark energy with $w=-1$. This assumption does not affect our results since the m_ν - w degeneracy is relevant only when combining CMB data with external measurements such as galaxy surveys or Lyα forest data (Hannestad 2005; Komatsu et al. 2008), unless we also allow for a direct dark energy – dark matter interaction (La Vacca et al. 2008).

In addition to the increase in uncertainties, the degeneracy between f_ν and $\omega_{\rm dm}$ leads to overestimate the dark matter density by $\sim 1\sigma$, as shown in figure 9 (also see Perotto et al. 2006).

Fitting for the relativistic degrees of freedom and Helium abundance significantly degrades the accuracy on most parameters, in particular on $\omega_{\rm dm}$, θ and $n_{\rm s}$, as shown by the results of table 9.

	70 - 143	70 - 100	70 - 217
$\omega_{\rm b}$	$1.7\times10^{-4}\,(1.06)$	1.54	0.87
$\omega_{\rm dm}$	$3.1\times10^{-3}\,(2.21)$	1.29	0.93
θ	$3.4\times10^{-3}\,(1.13)$	1.59	0.87
τ	$4.9\times10^{-3}\,(1.04)$	1.24	0.94
$n_{\rm s}$	$4.3\times10^{-3}\,(1.08)$	1.54	0.87
$\mathcal{A}_{\rm s}$	$1.0\times10^{-2}\,(1.06)$	1.23	0.94
f_ν	$< 7.2\times10^{-2}$	1.21	0.95
r	$< 0.034\,(1.13)$	2.32	0.83
σ_8	$5.2\times10^{-2}\,(7.76)$	1.15	0.96
H_0	$2.4\,(3.49)$	1.23	0.94

Table 8. Estimated accuracy for a ΛCDM + tensor + massive neutrinos model. We assume 3 families of massive neutrinos with fully degenerate mass eigenstates, and parametrise the massive neutrino contribution to the total energy density by f_ν. For f_ν we quote the 95% upper confidence limit. In parenthesis we report the ratio between estimates for this model and estimates for the base ΛCDM +r model for the same channels combination. As usual, results of columns 3 and 4 are quoted in units of uncertainties for the $70-143$ GHz channels.

[4] Due to the stochastic nature of MCMC methods, the 2σ upper limit on f_ν is determined with a 5% accuracy.

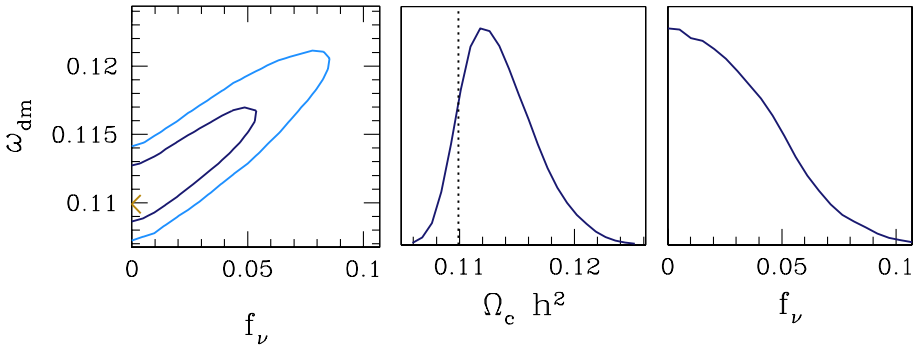

Figure 9. *Left*: Degeneracy between the neutrino fraction, f_ν and the total dark matter density, $\omega_{\rm dm}$. *Middle and Right*: Marginalised distribution over $\omega_{\rm dm}$ and f_ν, respectively. When marginalising over f_ν, the non – Gaussianity in the distribution of the neutrino fractions transfers to $\omega_{\rm dm}$, which leads to overestimating the dark matter density.

	70 - 143	70 - 217
$\omega_{\rm b}$	2.5×10^{-4} (1.60)	0.93
$\omega_{\rm dm}$	4.1×10^{-3} (2.93)	0.87
θ	1.1×10^{-3} (3.67)	0.85
τ	4.9×10^{-3} (1.04)	0.94
$n_{\rm s}$	8.9×10^{-3} (2.23)	0.92
$\mathcal{A}_{\rm s}$	1.3×10^{-2} (1.38)	0.90
$Y_{\rm He}$	1.7×10^{-2}	0.88
$N_{\rm eff}$	2.8×10^{-1}	0.87
r	< 0.029 (0.99)	0.86
σ_8	1.1×10^{-2} (1.64)	0.88
H_0	1.9 (2.75)	0.89

Table 9. As table 3, ΛCDM + tensor + $N_{\rm eff}$ + $Y_{\rm He}$. Assuming cleaning of the 217GHz channel would increase accuracy on most parameters by $\sim 10\%$. The third column reports the errors in units of the uncertainty for the base ΛCDM +r model, see table 3.

	70 - 143	70 - 100	70 - 217
$\omega_{\rm b}$	1.7×10^{-4}	1.42	0.88
$\omega_{\rm dm}$	1.4×10^{-3}	1.39	0.92
θ	3.0×10^{-3}	1.67	0.87
τ	5.0×10^{-3}	1.26	0.95
$n_{\rm s}$	4.0×10^{-3}	1.59	0.89
$n_{\rm run}$	5.8×10^{-3}	1.33	0.91
$\mathcal{A}_{\rm s}$	1.1×10^{-2}	1.25	0.95
r	< 0.037	2.20	0.83
σ_8	6.7×10^{-3}	1.30	0.93
H_0	6.9×10^{-1}	1.44	0.90

Table 10. Error forecasts for the ΛCDM + tensor + running model.

In agreement with Hamann et al. (2008) and Ichikawa et al. (2008), we find that Planck alone will be able to constrain $N_{\rm eff}$ to within $\sim 10\%$, even when simultaneously determining $Y_{\rm He}$.

3.4.3 *Running spectral index*

A power law is the simplest possible parametrisation for the power spectra of both scalar and tensor perturbations. However, several inflationary theories predicts small deviations from a pure power law, typically expressed as a logarithmic running of the spectral index, $n_{\rm run} = {\rm d}n_{\rm s}/{\rm d}log(k)$, at a suitable reference scale, $k_{\rm piv}$. Here we choose $k_{\rm piv} = 0.05{\rm Mpc}^{-1}$.

If only the 70 and 100 GHz Planck channels are available for cosmological parameter estimation, we find a moderate degeneracy between $n_{\rm s}$ and $n_{\rm run}$, similar to the one observed in actual WMAP5 data. This degeneracy results in an increase of the uncertainty on $n_{\rm s}$ by $\sim 10 - 15\%$ over what is obtained for our minimal parameter set. Including the 143 GHz channels substantially improves the determination of the high multipoles, which allows Planck to completely break this degeneracy, as shown in figure 10. Even with the inclusion of the 143 GHz channel, a minor degeneracy between $n_{\rm run}$ and τ remains, which partly propagates to $\mathcal{A}_{\rm s}$ and r. This degeneracy however, only slightly affects the constraints on these parameters. The remaining parameters are not significantly affected by the inclusion of $n_{\rm run}$ in the parameter set, regardless of the combination of frequencies considered.

3.4.4 *Tensor spectral index*

One of the most ambitious goals of Planck and other future CMB mission is the detection of primordial gravitational waves. In the minimal cosmological model considered here, with the tensor spectral index fixed to the input value $n_{\rm T} = 0$, r is not significantly degenerate with the other cosmological parameters. However, even if the tensor–to–scalar ratio is quite high $r \sim 0.15 - 0.20$, Planck will be able to constrain at most the first $10 - 15$ multipoles of the B mode spectra. It is then interesting to determine whether Planck will be able to simultaneously constrain r and $n_{\rm T}$.

We consider two fiducial models with $r = 0.01$ and $r = 0.10$, and $n_{\rm T}$ determined according to the single field inflation consistency relation $n_{\rm T} = -r/8$. In both cases, we also consider a non–zero running of the scalar spectral index $n_{\rm run} = -0.02$. The parameter set characterising our model is thus $\{\omega_{\rm b}, \omega_{\rm c}, \theta, \tau, n_{\rm s}, n_{\rm run}, \mathcal{A}_{\rm s}, n_{\rm T}, r\}$. Results of the analysis are summarised in table 11.

We find that for Planck the normalisation and spectral index are completely degenerate, as shown in figure 11. Allowing for $n_{\rm T}$ completely disrupts the instrument's capability for measuring r, even for moderate values of $r = 0.10$, as Planck does not have sufficient leverage on the B–modes to simultaneously constrain 2 tensor mode parameters. Errors on the remaining parameters are similar to those shown in table 10, implying that $n_{\rm T}$ is not significantly degenerate with the other parameters, in particular with $n_{\rm s}$ and $n_{\rm run}$.

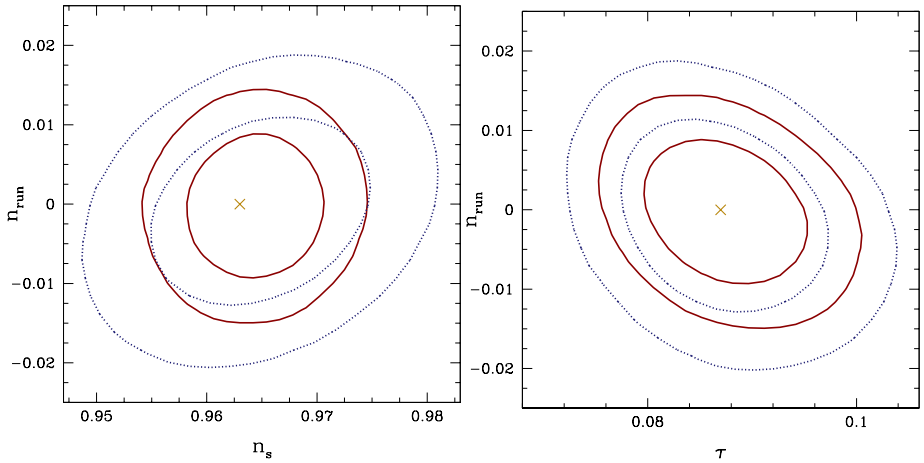

Figure 10. *Left:* 1- and 2-σ confidence regions in the $n_{\rm s} - n_{\rm run}$ plane, using $70 - 100$ Ghz channels (dashed lines) or $70 - 143$ GHz (solid lines) channels. Using just the 70 and 100 GHz channels allows for a mild degeneracy between the two parameters, which is broken if it is possible to clean the 143 GHz channel. *Right:* Confidence regions in the $\tau - n_{\rm run}$ plane. The contribution of the 143 GHz frequency does not help in breaking the mild degeneracy between the two parameters.

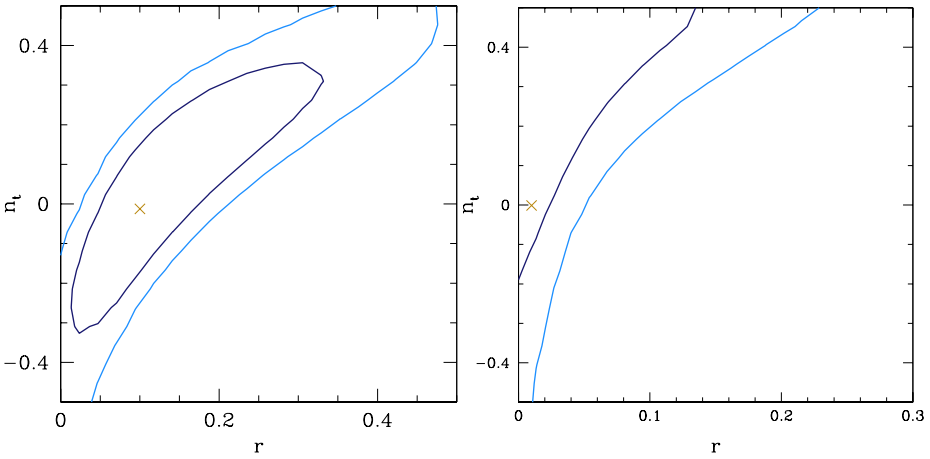

Figure 11. Degeneracy between the tensor–to–scalar ratio, r, and the tensor spectral index, n_t, for fiducial values $\{r = 0.10, n_t = -0.0125\}$ (left) and $\{r = 0.01, n_t = -0.00125\}$ (right). Even for moderate values $r \sim 0.10$, Planck does not have sufficient leverage on the B–modes to simultaneously constrain r and n_t.

4 PLANCK AS SUPPORT FOR OTHER MISSIONS

In the previous section, we have seen that Planck's performance for wider parameter spaces is often limited by degeneracies inherent to the CMB data. Further improvement on parameter constraints will come not from improved CMB data, but by combination with other experimental techniques. In this section, we will use the Fisher matrix formalism to illustrate constraints for proposed galaxy surveys in combination with WMAP or Planck. The Fisher matrix technique has been discussed in detail by many authors, e.g. Eisenstein et al. (1999), and we direct the interested reader to Pritchard & Pierpaoli (2008) for further information on our Fisher matrix methodology. Throughout we will assume usage of the Planck's 70-143 channels for cosmological constraints and consider WMAP5 and WMAP8 modelled by simply increasing the sensitivity by the longer integration time.

4.1 Dark energy

Dark energy is, perhaps, the most challenging unsolved problem facing modern cosmology. However, as we saw in §3.4.1, there is a strong geometrical degeneracy between Ω_Λ, $\Omega_{\rm K}$, and w present in the CMB. It is therefore necessary to combine CMB information with distance measurements in the low redshift Universe in order to break this degeneracy and constrain dark energy precisely.

A promising technique is the measurement of baryon acoustic oscillations (BAO) in the galaxy power spectrum. Since the wavelength of the BAO is set by the same sound horizon measured in the CMB the BAO can be used as a "standard ruler" to measure distances. CMB information plays a dual role by calibrating this standard ruler and providing a distance measurement at high redshifts.

Here we consider constraints from a spectroscopic BAO galaxy survey of 10,000 sq. deg. spanning redshifts $z = 0.5 - 2$. This is a stage IV space BAO mission in the language of Albrecht et al. (2006) and a possible configuration for the proposed JDEM mission. The 68% confidence ellipses in the $\Omega_\Lambda - w_0$ plane

	$r = 0.01$	$r = 0.10$
$\omega_{\rm b}$	1.7×10^{-4}	1.8×10^{-4}
$\omega_{\rm dm}$	1.4×10^{-3}	1.4×10^{-3}
θ	3.1×10^{-3}	3.1×10^{-3}
τ	5.2×10^{-3}	5.2×10^{-3}
$n_{\rm s}$	4.0×10^{-3}	4.1×10^{-3}
$n_{\rm run}$	5.8×10^{-3}	6.1×10^{-3}
$\mathcal{A}_{\rm s}$	1.1×10^{-2}	1.1×10^{-2}
r	< 0.16	< 0.38
$n_{\rm T}$	0.2	0.2
σ_8	6.8×10^{-3}	6.9×10^{-3}
H_0	7.0×10^{-1}	7.0×10^{-1}

Table 11. Error forecasts for the ΛCDM + running + tensor spectral index model. Second columns shows results for a fiducial model with $r = 0.01$, column 3 refer to $r = 0.10$. In both cases, we considered the $70 - 143$ GHz channels specifications.

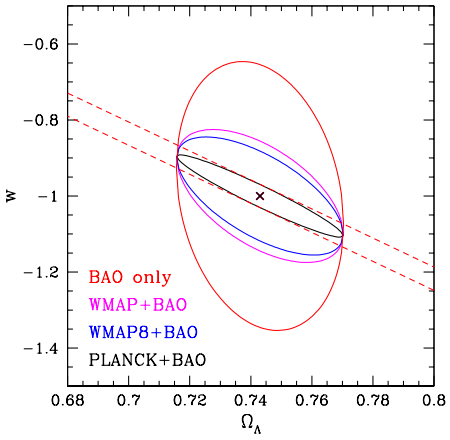

Figure 12. 68% confidence ellipses in the $\Omega_\Lambda - w_0$ plane for BAO in combination with CMB experiments. Dashed curve indicates the constraint from Planck alone with a weak prior on Ω_Λ.

for this experiment are shown in Figure 12 and summarised in Table 12, where the constraints have been calculated with a flat prior and include representative systematic errors on distance measures to each redshift bin and account for non-linear smoothing of the acoustic features according to the Fisher matrix prescription outlined in the Dark Energy Task Force (DETF) report (Albrecht et al. 2006). It is readily seen that the combination of distance measurements at low and high redshift leads to tight constraints on dark energy parameters. The low redshift data is essential in fixing the matter content of the Universe (or equivalently h) breaking the geometric degeneracy.

If we expand our parameter set to allow for evolving dark energy with equation of state $w(a) = w_0 + (1 - a)w_a$ (Chevallier & Polarski 2001) the improvement from adding CMB can be quantified by the DETF figure of merit (FoM), which is defined to be proportional to the inverse area contained within the $w_0 - w_a$ error ellipse. These are listed in Table 12. WMAP8 provides a 16% increase in DETF FoM over WMAP5, while Planck is a ~ 2 fold increase in DETF FoM over WMAP5. Thus the goal of making precision measurements of dark energy very much require precision CMB observations at the Planck level.

Table 12. Dark energy constraints for BAO + CMB

Experiment	$\sigma(\Omega_\Lambda)$	$\sigma(w_0)$	relative FoM
BAO only	0.02	0.23	1
BAO + WMAP5	0.02	0.12	9.6
BAO + WMAP8	0.02	0.10	11.1
BAO + Planck	0.02	0.07	20.3

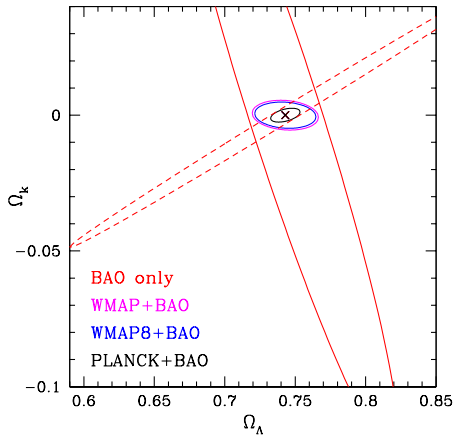

Figure 13. 68% confidence ellipses in the $\Omega_\Lambda - \Omega_{\rm K}$ plane for BAO in combination with CMB experiments. Dashed curve indicates the constraint from Planck alone.

4.2 Curvature

Since $\Omega_{\rm K}$ is subject to the same geometric degeneracy as w and Ω_Λ constraining the curvature is vital for obtaining precision dark energy constraints. Typically once constraints at the level of $\Omega_{\rm K} \sim 2 \times 10^{-3}$ are reached this degeneracy is broken (Knox et al. 2006).

We apply the same BAO experiment as in the previous subsection to calculate the constraints shown in Figure 13. The strong degeneracy in the CMB data and BAO data have very different alignments and in combination lead to constraints at the level of $\Omega_{\rm K} \sim$ few $\times 10^{-3}$. Table 13 summarises the results.

Including both a variable dark energy equation of state and curvature does not degrade these curvature constraints significantly. Further, since the curvature is well constrained, we recover constraints on Ω_Λ and w degraded by $\lesssim 5\%$ from those of Table 12 that were calculated with a flat prior. This illustrates that the degeneracy between curvature and dark energy parameters is broken by these experiments.

4.3 Inflationary parameters

Constraining inflationary parameters is of paramount importance in pointing the way towards a theoretical understanding of first fractions of a second of the Universe's evolution. The CMB is sensitive

Table 13. Curvature constraints for BAO + CMB

Experiment	$\sigma(\Omega_\Lambda)$	$\sigma(\Omega_{\rm K})$
BAO only	0.05	0.08
BAO + WMAP5	0.015	0.0037
BAO + WMAP8	0.014	0.0032
BAO + Planck	0.0066	0.0017

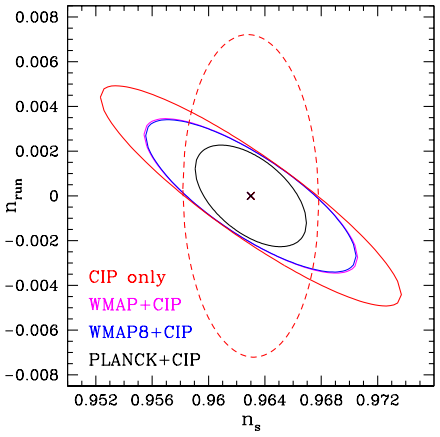

Figure 14. Effect of CMB support on CIP for inflation constraints in the $n_{\rm s} - n_{\rm run}$ plane. Dashed curve indicates the constraint from Planck alone.

to the shape of the primordial power spectrum over wavenumbers ranging from $k = 0.002 - 0.2h\,{\rm Mpc}^{-1}$, since Silk damping effectively erases information about smaller scales. Improving constraints on the tilt $n_{\rm s}$ and running α of the primordial power spectrum will require combining CMB information with information derived from the matter power spectrum, which extends to smaller scales increasing the lever arm (Adshead & Easther 2008). Precision measurements of $n_{\rm s}$, $n_{\rm run}$, and r will begin to allow reconstruction of the inflaton potential.

There are currently three techniques proposed for measuring small scale power: galaxy surveys, the Lyman-alpha forest, and redshifted 21 cm experiments. The first two techniques are subject to systematic uncertainties arising from the non-linear evolution of the matter power spectrum, while the latter is still in its infancy and may be affected by the imprint of reionisation on the intergalactic medium (IGM) (Furlanetto et al. 2006). Perhaps the most promising approach will be high redshift ($z = 2 - 6$) galaxy surveys, which probe the matter power spectrum when the scale of non-linearities is small and so may extend to $k \sim 2h$ Mpc^{-1} or larger. For this analysis, we consider the proposed *Cosmic Inflation Probe* (CIP), a space based mission to survey galaxies in Hα over the range $z = 2 - 6.5$ (Melnick et al. 2004), and assess the importance of CMB support for placing constraints in the $n_{\rm s} - n_{\rm run}$ plane. We assume that CIP will survey 1000 sq. deg. on the sky detecting 200 million galaxies. CIP is designed to produce an error ellipse for inflationary constraints that is comparable to that obtained using Planck alone. Since they cover very different scales the combination is expected to yield precise constraints on inflation.

Error ellipses for CIP in combination with CMB experiments are shown in Figure 14. Although there is no significant degeneracy present in the CMB data, for CIP there is a strong degeneracy between $n_{\rm s}$ and $n_{\rm run}$, since CIP predominantly measures the power spectrum on scales smaller than the pivot point $k_{\rm pivot} = 0.05\,{\rm Mpc}^{-1}$. Planck data provides tight constraints on $n_{\rm s}$ partially breaking this degeneracy and leading to much improved constraints on $n_{\rm run}$.

It is apparent that increasing the observation time from 5 to 8 years for WMAP shows little improvement in the inflationary constraints from the combination with CIP, Planck is needed. Constraints are listed in Table 14. We may use the generalisation of the DETF figure of merit to the inflationary parameters

Table 14. Inflationary constraints for CIP + CMB

Experiment	$\sigma(n_{\rm s})$	$\sigma(n_{\rm run})$	relative FoM
CIP only	0.007	0.0032	1
CIP + WMAP5	0.005	0.0022	1.47
CIP +WMAP8	0.0049	0.0022	1.49
CIP +Planck	0.0026	0.0015	3.07

(Adshead & Easther 2008) to quantify this. For this figure of merit, both WMAP5 and WMAP8 provide a factor of 1.5 increase over CIP alone, while Planck improves the inflationary FoM by a factor of 3.0. The combination of Planck+CIP measures $n_{\rm run}$ at the level of 10^{-3} (in agreement with Takada et al. 2006), which is roughly the largest value consistent with simple slow roll inflation models and the current constraints on $n_{\rm s}$ and is also comparable with that of some more exotic inflationary models (e.g. Bastero-Gil et al. 2003; Chung et al. 2003).

4.4 Neutrino masses

As discussed earlier, the CMB displays a strong degeneracy between $\omega_{\rm dm}$ and f_ν since both affect the energy density in non-relativistic matter before decoupling in a similar manner. By adding low red-shift information where neutrinos have become non-relativistic this degeneracy may be broken (Lesgourgues & Pastor 2006, for a review of neutrino physics, see).

In a similar fashion to constraining inflation, constraints on neutrino mass benefit from constraints on the matter power spectrum on small scales. In the relatively near future, surveys such as the *Large Synoptic Survey Telescope* [5] (LSST) are likely to survey large numbers of galaxy at $z < 3$ with photometric redshifts. These are expected to greatly improve the constraints on neutrino masses. A similar analysis taking into account the combination of CIP and Planck was performed by Takada et al. (2006). Neutrinos show themselves in the matter power spectrum as a suppression of power on small scales where relativistic neutrinos are able to freestream out of gravitational potentials smoothing the distribution of matter. If neutrinos have mass then at late times they become non-relativistic and begin to cluster in the gravitational potentials set by the dominant dark matter component. Since neutrinos of different masses would become non-relativistic at different times the amplitude of power on small scales as a function of redshift is a useful probe of neutrino mass.

Figure 15 shows constraints in the $\omega_{\rm dm} - f_\nu$ plane for $f_\nu = 0.01$, corresponding to a total neutrino mass of $M_\nu = 0.1\,{\rm eV}$. We assume that LSST measures galaxies with photometric redshifts (with uncertainty $\sigma_z = 0.04$) in six redshift bins over the range $z = 0.5 - 3$. We model the observed density of galaxies as $n_g(z) = 640 z^2 e^{-z/0.35}\,{\rm arcmin}^{-2}$. Note that the uncertainty is to some extent driven by the photometric redshifts. If LSST achieved $\sigma_z = 0.02$ then the constraints would be significantly improved and most of the constraining power would come from LSST alone.

LSST alone does a reasonable job of measuring f_ν, but by placing a tight constraint on $\omega_{\rm dm}$ it also breaks the degeneracy present in the CMB data leading to a much tighter constraint on f_ν. Once Planck is added to LSST a constraint on M_ν at the level of 0.05 eV is achievable - sufficient for a detection and comparable

[5] http://www.lsst.org/Science/DETF.shtml

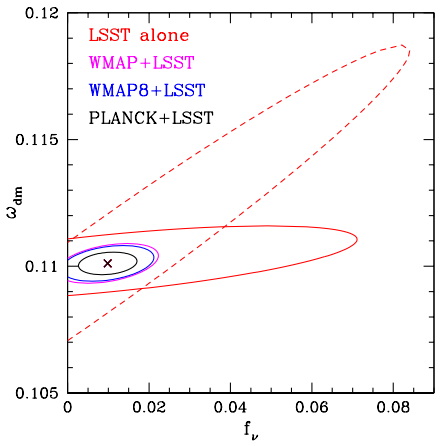

Figure 15. Effect of CMB support on LSST for neutrino mass constraints in the $\omega_{dm} - f_\nu$ plane. Dashed curve indicates the constraint from Planck alone.

Table 15. Neutrino mass constraints for LSST + CMB

Experiment	$\sigma(\omega_{dm})$	$\sigma(f_\nu)$
LSST only	0.00097	0.04
LSST + WMAP5	0.00052	0.0082
LSST +WMAP8	0.00046	0.0075
LSST +Planck	0.00029	0.0047

to the value expected from the observed neutrino mass splittings (Fogli et al. 2008).

5 CONCLUSIONS

In this paper we performed a MCMC estimate of cosmological constraints expected from the upcoming Planck data. The actual contribution by Planck to cosmology will ultimately depend on a number of factors, especially on systematics control and foreground cleaning. In this work we adopted a simple approach to foreground cleaning. We supposed that a number of frequencies will be used to fully remove foregrounds from the remaining channel, which are then used to constrain the cosmological parameters, and discussed how such constraints depend on the frequencies used.

As a general result, we find that a combination of 70, 100, and 143 GHz channels allows Planck to achieve $85 - 90\%$ of its potential, corresponding to a factor 3 - 4 improvement over WMAP 5 year results for the minimal ΛCDM model. Adding the remaining LFI frequencies as well as the 217 GHz channel essentially accounts for all of Planck capabilities in terms of cosmological parameters. Higher frequencies, while useful for foregrounds control and additional science, do not significantly increase the accuracy on the main parameters.

For the cosmology currently preferred by WMAP5 data, Planck will provide a cosmic variance limited determination of the temperature power spectrum up to $\ell \simeq 1000$, while the signal–to–noise ratio will be unity around $\ell \simeq 1600 - 1800$ depending on the channels considered. This high–ℓ temperature information is essential for determination of $n_{\rm s}$ and $\Omega_{\rm b}$ (30-40% improvement wrt constraints obtaining including only multipoles up to $\ell_{max} = 800$). Multipoles in the range $2000 \lesssim \ell \lesssim 2500$ only provide a few percent contribution to the accuracy on cosmological parameters, however this estimate does not consider gravitational lensing and effects like beam systematics which introduce correlation between different multipoles. The impact of multipoles in this range over the final Planck constraints will strongly depend on the relevance of these effects. Future experiments, achieving a cosmic variance limited measurement of the TT power spectrum up to $\ell \simeq 2500$ will improve Planck constraints on $\omega_{\rm b}$, $n_{\rm s}$ and θ by $\sim 30 - 40\%$. We find that having a beam slightly bigger than that quoted degrades constraints by $\sim 10\%$ on $n_{\rm s}$ and $\Omega_{\rm b}$. However, adopting a slightly wrong value for the FWHM in the data analysis does bias the results for several parameters significantly.

Planck will provide a factor of ~ 9 improvement over WMAP in determining the upper limit for the tensor–scalar–ratio. Losing the polarization information from the 143 GHz channel would degrade this by a factor of two. Being unable to constrain B–modes, as results of foreground contamination would also degrade the error on r by a factor of ~ 2, with a slight dependence on the fiducial value of the tensor–to–scalar ratio. Planck alone will be unable to constrain the tensor spectral index $n_{\rm T}$. Further, if the full 70–143 GHz range is available the degeneracy between $n_{\rm s}$ and $n_{\rm run}$ is broken allowing constraints on both a factor of five beyond those achieved by WMAP. Taken together, Planck will greatly improve our constraints on the inflationary parameter space.

Significant degeneracies remain in the Planck data due to intrinsic degeneracies in CMB. The strong geometric degeneracy in the angular diameter distance determination remains, although errors on parameters like $\Omega_{\rm K}$ and w will improve by a factor 2 compared to WMAP5 thanks to a better determination of the angular scale of the CMB acoustic peaks. Neutrino properties are much better constrained (especially $N_{\rm eff}$ for which the current degeneracy is totally removed), but a strong degeneracy between f_ν and $\omega_{\rm dm}$ remains and considering neutrinos in the analysis increases the estimated error on σ_8 by a factor ~ 8.

We have verified that all of these intrinsic degeneracies can be broken by the addition of extra low-redshift data sets. Large scale structure measurements provide a measurement of Ω_Λ breaking the geometric degeneracy between Ω_Λ, w, and $\Omega_{\rm K}$ present in CMB data alone. For a JDEM type mission, Planck improves the constraint on w and $\Omega_{\rm K}$ by almost a factor of two over using WMAP5 data. Although Planck does not see a strong degeneracy between $n_{\rm s}$ and $n_{\rm run}$, galaxy surveys like CIP, which probe smaller scales, do. Combining CIP with Planck breaks this degeneracy leading to constraints on the running that are a factor of 2 better than from Planck alone. Finally, by measuring the non-relativistic matter content today, galaxy surveys such as LSST break the degeneracy between ω_m and f_ν improving constraints on f_ν by an order of magnitude to the level of the observed mass splittings. On all of these parameters using Planck offers at least a $50 - 100\%$ improvement over WMAP5, illustrating its importance as a support for other data sets.

ACKNOWLEDGMENTS

EP is and NSF–ADVANCE fellow (AST–0649899) also supported by JPL SURP award 1314616. LPLC and EP were supported by NASA grant NNX07AH59G and Planck subcontract 1290790 for this work, and would like to thank Caltech for hospitality during this period. JRP is supported by NASA through Hubble Fellowship grant HST-HF-01211.01-A awarded by the Space Telescope Science Institute, which is operated by the Association of Universities for Research in Astronomy, Inc., for NASA, under contract NAS 5-26555. We acknowledge the use of the CosmoMC, PICO

and HEALPix packages. The authors thanks Kevin Huffenberger and Brendan Crill for stimulating discussion on beams effect.

REFERENCES

Adshead P., Easther R., 2008, ArXiv e-prints, 802
Albrecht A., Bernstein G., Cahn R., Freedman W. L., Hewitt J., Hu W., Huth J., Kamionkowski M., Kolb E. W., Knox L., Mather J. C., Staggs S., Suntzeff N. B., 2006, ArXiv Astrophysics e-prints
Amendola, L. 2000, Phys. Rev. D, 62, 043511
Balbi, A. 2007, New Astronomy Review, 51, 281
Bastero-Gil M., Freese K., Mersini-Houghton L., 2003, Phys. Rev. D, 68, 123514
Betoule, M. et al. in preparation
Bock, J., et al. 2008, arXiv:0805.4207
Bond, J. R., Contaldi, C., Lewis, A., & Pogosyan, D. 2004, International Journal of Theoretical Physics, 43, 599
Brax, P. H., & Martin, J. 1999, Physics Letters B, 468, 40
Brown, M. L., Castro, P. G., & Taylor, A. N. 2005, MNRAS, 360, 1262
Burigana, C., Popa, L. A., Finelli, F., Salvaterra, R., De Zotti, G., & Mandolesi, N. 2004, arXiv:astro-ph/0411415
Caldwell, R. R., Dave, R., & Steinhardt, P. J. 1998, Physical Review Letters, 80, 1582
Chevallier, M., & Polarski, D. 2001, International Journal of Modern Physics D, 10, 213
Chung D. J. H., Shiu G., Trodden M., 2003, Phys. Rev. D, 68, 063501
Colombo, L. P. L., & Pierpaoli, E. 2008, arXiv:0804.0278
Crill, B. P., et al. 2008, arXiv:0807.1548
Dunkley, J., et al. 2008, arXiv:0803.0586
Eisenstein D. J., Hu W., Tegmark M., 1999, ApJ, 518, 2
Elgarøy, O., & Multamäki, T. 2007, A&A, 471, 65
Fendt, W. A., & Wandelt, B. D. 2007, ApJ, 654, 2
Fogli G. L., Lisi E., Marrone A., Melchiorri A., Palazzo A., Rotunno A. M., Serra P., Silk J., Slosar A., 2008, Phys. Rev. D, 78, 033010
Furlanetto S. R., Oh S. P., Briggs F. H., 2006, Phys. Rep., 433, 181
Gold, B., et al. 2008, arXiv:0803.0715
Górski, K. M., Hivon, E., Banday, A. J., Wandelt, B. D., Hansen, F. K., Reinecke, M., & Bartelmann, M. 2005, ApJ, 622, 759
Gratton, S., Lewis, A., & Efstathiou, G. 2008, Phys. Rev. D, 77, 083507
Hamann, J., Lesgourgues, J., & Mangano, G. 2008, Journal of Cosmology and Astro-Particle Physics, 3, 4
Hamimeche, S., & Lewis, A. 2008, Phys. Rev. D, 77, 103013
Hannestad, S. 2005, Physical Review Letters, 95, 221301
Hivon, E., Górski, K. M., Netterfield, C. B., Crill, B. P., Prunet, S., & Hansen, F. 2002, ApJ, 567, 2
Huey, G., & Wandelt, B. D. 2006, Phys. Rev. D, 74, 023519
Knox, L., & Turner, M. S. 1994, Physical Review Letters, 73, 3347
Komatsu, E., et al. 2008, arXiv:0803.0547
Ichikawa, K., Fukugita, M., & Kawasaki, M. 2005, Phys. Rev. D, 71, 043001
Ichikawa, K., Sekiguchi, T., & Takahashi, T. 2008, arXiv:0803.0889
Knox L., Song Y.-S., Zhan H., 2006, ApJ, 652, 857
La Vacca, G., & Colombo, L. P. L. 2008, Journal of Cosmology and Astro-Particle Physics, 4, 7
La Vacca, G., Bonometto, S. A., & Colombo, L. P. L. 2008, arXiv:0810.0127
Lewis, A., & Bridle, S. 2002, Phys. Rev. D, 66, 103511
Lewis, A., Challinor, A., & Turok, N. 2002, Phys. Rev. D, 65, 023505
Lewis, A. 2005, Phys. Rev. D, 71, 083008
Lesgourgues, J., & Pastor, S. 2006, Phys. Rep., 429, 307
Linde, A., & Mezhlumian, A. 1995, Phys. Rev. D, 52, 6789
Lyth, D. H. D. H., & Riotto, A. A. 1999, Phys. Rep., 314, 1
Mainini, R., Colombo, L. P. L., & Bonometto, S. A. 2005, ApJ, 632, 691
Melnick G. J., Fazio G. G., Tolls V., Jaffe D. T., Gebhardt K., Bromm V., Komatsu E., Woodruff R. A., 2004, in Bulletin of the American Astronomical Society Vol. 36 of Bulletin of the American Astronomical Society, The Cosmic Inflation Probe (CIP) - Constraining the Physics of Inflation. pp 1509
Mortonson, M. J., & Hu, W. 2008, ApJ, 672, 737
Mukherjee, P., Kunz, M., Parkinson, D., & Wang, Y. 2008, arXiv:0803.1616
Percival, W. J., & Brown, M. L. 2006, MNRAS, 372, 1104
Perotto, L., Lesgourgues, J., Hannestad, S., Tu, H., & Y Y Wong, Y. 2006, Journal of Cosmology and Astro-Particle Physics, 10, 13
Pierpaoli, E. 2003, MNRAS, 342, L63
Pritchard J. R., Pierpaoli E., 2008, Phys. Rev. D, 78, 065009
Ratra, B., & Peebles, P. J. E. 1988, Phys. Rev. D, 37, 3406
Samtleben, D., Staggs, S., & Winstein, B. 2007, Annual Review of Nuclear and Particle Science, 57, 245
Serra, P., Cooray, A., Amblard, A., Pagano, L., & Melchiorri, A. 2008, Phys. Rev. D, 78, 043004
Smith, S., Challinor, A., & Rocha, G. 2006, Phys. Rev. D, 73, 023517
Takada, M., Komatsu, E., & Futamase, T. 2006, Phys. Rev. D, 73, 083520
Tegmark, M., & de Oliveira-Costa, A. 2001, Phys. Rev. D, 64, 063001
The Planck Collaboration 2006, arXiv:astro-ph/0604069
Vergani, L., Colombo, L. P. L., La Vacca, G., & Bonometto, S. A. 2008, arXiv:0804.0285
Xia, J.-Q., Li, H., Zhao, G.-B., & Zhang, X. 2007, arXiv:0708.1111
Wetterich, C. 1988, Nuclear Physics B, 302, 645
White, M. 2006, New Astronomy Review, 50, 938